JACS
JOURNAL OF THE AMERICAN CHEMICAL SOCIETY
Communication
pubs.acs.org/JACS

Pruning the ALS-Associated Protein SOD1 for in-Cell NMR

Jens Danielsson,*[,†] Kohsuke Inomata,[‡,§] Shuhei Murayama,[‡] Hidehito Tochio,[‡] Lisa Lang,[†] Masahiro Shirakawa,*[,‡] and Mikael Oliveberg*[,†]

[†]Department of Biochemistry and Biophysics, Arrhenius Laboratories of Natural Sciences, Stockholm University, S-106 91 Stockholm, Sweden

[‡]Department of Molecular Engineering, Graduate School of Engineering, Kyoto University, Katsura, Kyoto 615-8510, Japan

[§]Laboratory for Cell Dynamics Observation, Quantitative Biology Center, RIKEN, OLABB, Osaka University 6-2-3, Furuedai, Suita, Osaka 565-0874, Japan

Supporting Information

ABSTRACT: To efficiently deliver isotope-labeled proteins into mammalian cells poses a main challenge for structural and functional analysis by in-cell NMR. In this study we have employed cell-penetrating peptides (CPPs) to deliver the ALS-associated protein superoxide dismutase (SOD1) into HeLa cells. Our results show that, although full-length SOD1 cannot be efficiently internalized, a variant in which the active-site loops IV and VII have been truncated (SOD1$^{\Delta IV\Delta VII}$) yields high cytosolic delivery. The reason for the enhanced delivery of SOD1$^{\Delta IV\Delta VII}$ seems to be the elimination of negatively charged side chains, which alters the net charge of the CPP-SOD1 complex from neutral to +4. The internalized SOD1$^{\Delta IV\Delta VII}$ protein displays high-resolution in-cell NMR spectra similar to, but not identical to, those of the lysate of the cells. Spectral differences are found mainly in the dynamic β strands 4, 5, and 7, triggered by partial protonation of the His moieties of the Cu-binding site. Accordingly, SOD1$^{\Delta IV\Delta VII}$ doubles here as an internal pH probe, revealing cytosolic acidification under the experimental treatment. Taken together, these observations show that CPP delivery, albeit inefficient at first trials, can be tuned by protein engineering to allow atomic-resolution NMR studies of specific protein structures that have evaded other in-cell NMR approaches: in this case, the structurally elusive apoSOD1 barrel implicated as precursor for misfolding in ALS.

Considerable effort has been invested to determine how the properties of proteins are affected by the complex and spatially restricted interior of living cells.[1] Of particular interest here is how mammalian cells modulate protein misfolding and template-directed aggregation processes associated with neurodegenerative disease, an area that is yet poorly understood.[2,3] An atomic-resolution tool for elucidating such *in vivo* modulation is NMR.[4,5] In-cell NMR has successfully been applied to bacteria where high intracellular loading of isotope-labeled protein target is accomplished by overexpression,[6,5] even allowing direct in-cell spectral assignment and structural determination. For mammalian cells two general strategies are used, with accompanying arguments *pro et contra*: overexpression[7] or delivery of externally isotope-labeled protein. NMR detection is often challenged by insufficient levels of internalized protein.[8]

Essentially, two methods have been employed for internalization of externally labeled protein: diffusion through toxin-induced pores[9] or delivery by cell-penetrating peptides (CPPs).[10] For some proteins these strategies work beautifully, whereas for others they fail completely. In this communication we focus on protein delivery into mammalian cells by CPPs and demonstrate that success in terms of high-resolution in-cell NMR spectra can be achieved by protein engineering. Our model system is the immunoglobulin-like protein superoxide dismutase 1 (SOD1) associated with pathologic aggregation in the neurodegenerative disease amyotropic lateral sclerosis (ALS) (Figure 1). Based on the earlier observations by Banci

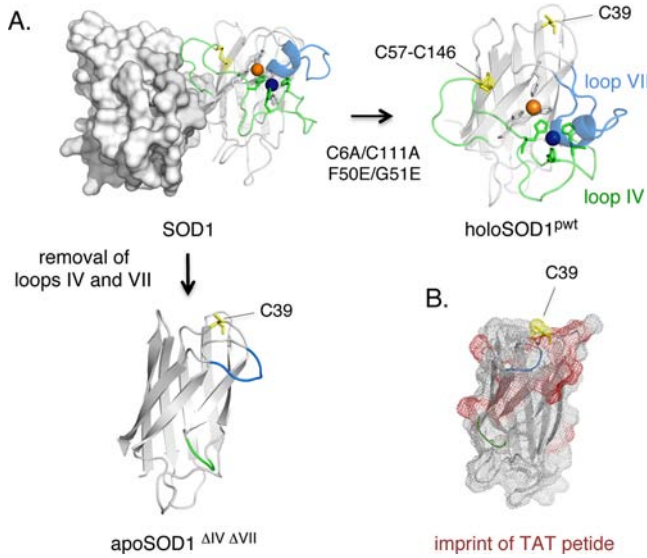

Figure 1. (A) Homodimeric SOD1, the monomeric variant holoSOD1^{pwt}, harboring zinc (blue sphere) and copper (orange sphere) and the monomeric barrel SOD1$^{\Delta IV\Delta VII}$ obtained by truncation of the functional loops IV (green) and VII (blue). (B) SOD1$^{\Delta IV\Delta VII}$ showing the chemical-shift imprint of TAT attached at C39. Chemical shift differences >75 ppb are in red.

Received: May 3, 2013
Published: July 2, 2013

   dx.doi.org/10.1021/ja404425r | J. Am. Chem. Soc. 2013, 135, 10266−10269

et al. that SOD1 can be detected by in-cell NMR in *E. coli* and human embryonic kidney cells following metalation of overexpressed wild-type protein,[7,11] we chose here the well-characterized holoSOD1 monomer (holoSOD1^{pwt}) as base for our study (S1). The advantage of this wild-type-like, structurally stable, and enzymatically active SOD1 variant[12−14] is that it is devoid of the free cysteines C6 and C111, which could otherwise interfere with the disulfide-mediated attachment of CPPs. Also, because it is monomeric, it allows the construction of unimolecular protein−CPP complexes with short rotation-correlation times, which assures NMR detectability even under conditions of high solution crowding and decreased molecular diffusion. Following the protocols by Shirakawa and co-workers,[10] the activated CPP R8 was selectively linked to ^{15}N labeled holoSOD1^{pwt} by the surface mutation T39C (Figure 1) and subjected to confluent HeLa cells preconditioned for CPP delivery, after 'recovery', wash, and transfer of the cells to the NMR apparatus. However, these samples produce only very weak HMQC spectra showing folded holoSOD1^{pwt} at an effective concentration of <3 μM (S2). The spectra originate solely from holoSOD1^{pwt} outside the cells: no signal was obtained from either the supernatant or the cell lysate (S2). On this basis, we conclude that the R8-holoSOD1^{pwt} complex does not efficiently translocate into HeLa cells. To see if delivery was prevented by the holo protein's high structural integrity,[13,14] i.e., resistance to transiently unfold or structurally adjust during internalization, the experiments were repeated with the less stable and more plastic monomeric SOD1^{pwt} without coordinated metals, apoSOD1^{pwt}.[14] The result was the same: the protein fails to produce in-cell NMR spectra (S2). To finally eliminate the possibility that the native disulfide linkage C57−C146 complicates delivery by scrambling with the R8−C39 attachment, we tried also with the fully cysteine-depleted variant holoSOD^{CallA} [15] but, again, without effect on the result (S2).

Although the mechanism of protein delivery with CPPs is not fully understood, a key molecular determinant is net charge;[16] as long as the CPP carries a sufficient amount positive charge to override the net charge of the cargo, its detailed amino-acid composition seems to be of secondary importance. Positive charge of C-terminal transport signals drives also internalization of pathogens,[17] and even artificially, the rather bulky green fluorescence protein is observed to spontaneously penetrate cells upon mutating its global charge from −6.2 to +36.[18] In this context it is notable that, because SOD1 like most other proteins is negatively charged, the net charge of the R8−SOD1^{pwt} complex sums up to ±0 (S3). To examine if this counterbalance opposes cell delivery, we reduced the SOD1 charge by truncation of the active-site loops IV and VII (SOD1$^{\Delta IV\Delta VII}$, Figure 1). Notably, this truncated species, representing the 'naked' SOD1 scaffold, is found to comprise all of the structural components critical for *in vitro* aggregation.[19,20] The truncation affects just marginally the stability and dynamic properties of the SOD1 structure[14,20] but alters the net charge of the peptide−protein complex to +5.4 (S3). As a result, the efficiency of CPP delivery increases radically, yielding highly dispersed in-cell NMR spectra of the SOD1$^{\Delta IV\Delta VII}$ molecule (Figure 2). Subsequent centrifugation and lysis of the cell sample showed that the entire NMR signal this time originated from internalized protein (Figure 2, S4). The intracellular concentration of SOD1$^{\Delta IV\Delta VII}$ was roughly estimated to 20 μM from NMR signal intensity. As control, the experiments were repeated with the TAT peptide, producing

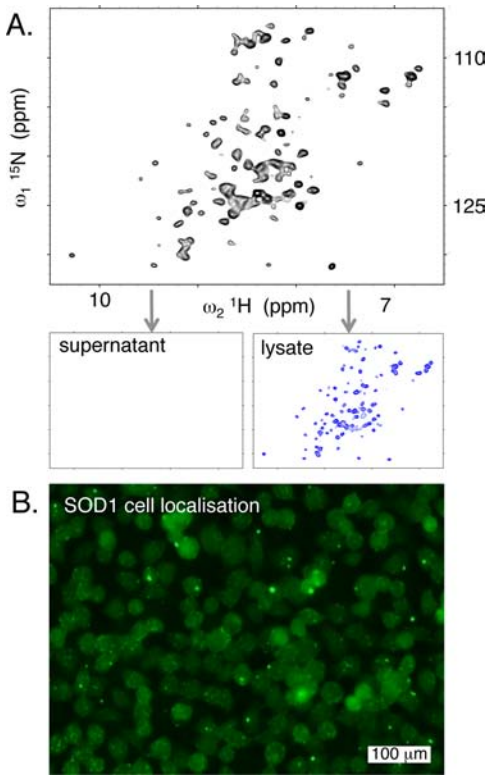

Figure 2. (A) In-cell HMQC spectra of SOD1$^{\Delta IV\Delta VII}$ with sample supernatant and lysed pellet controls. (B) Cytosolic localization of SOD1$^{\Delta IV\Delta VII}$ after TAT delivery of ALEXA labeled protein.

indistinguishable results (Table 1). Finally, fluorescence labeling of the TAT− SOD1$^{\Delta IV\Delta VII}$ complex indicated diffuse cytosolic localization, consistent with earlier results on ubiquitin using the same delivery protocol[10] (Figure 2).

Table 1. Stability, Net Charge, And Results

protein construct	stability[a] $\Delta G_{U/F}$ (kcal/mol)	net charge at pH 7	in-cell signal	viability[b] (%)
holoSOD1^{pwt}−R8	7.11	0.6	no	72
apoSOD1^{pwt}−R8	2.24	0.6	no	80
holoSOD1^{CallA}−R8	7.36	0.7	no	96
SOD1$^{\Delta IV\Delta VII}$−R8	3.68	5.4	yes	94
SOD1$^{\Delta IV\Delta VII}$−TAT	3.68	5.4	yes	96

[a]Determined from $\Delta G_{U/F} = -2.3RT(\log k_f - \log k_u)$ (S7). [b]Viability after 3h in the NMR tube. The viability of apoSOD1$^{\Delta IV\Delta VII}$ after 6 h is still high at 90%, indicating that the cells are quite resistant to the experimental conditions in the NMR tube.

Attachment of the CPP to an alternative position by the mutation S75C produces indistinguishable result (S5). The disulfide-mediated attachment of the TAT peptide was verified by NMR chemical shifts, showing that the peptide wraps diffusely around the SOD1$^{\Delta IV\Delta VII}$ surface (Figure 1, S6). Following delivery and in-cell NMR analysis, the SOD1$^{\Delta IV\Delta VII}$ material recovered from lysed HeLa cells displays no signs of these TAT-induced shifts. The disulfide anchor or the CPP seems thus to dissociate from the protein upon transfer into the reducing cytosol of the HeLa cells, further supporting the conclusion that the NMR spectra in Figure 2 are indeed from internalized material. In contrast, delivery into the more

dx.doi.org/10.1021/ja404425r | J. Am. Chem. Soc. 2013, 135, 10266−10269

oxidative interior of endosomes would leave the disulfide anchor intact.[21] Due to general signal broadening, direct verification of CPP dissociation from in-cell NMR data is less clear-cut. Even so, the majority of involved chemical-shift changes indicates that the CPP is lost immediately upon cell delivery, in particular the shift of V14 where the spectral overlap is minimal (Figure 3). As an additional control,

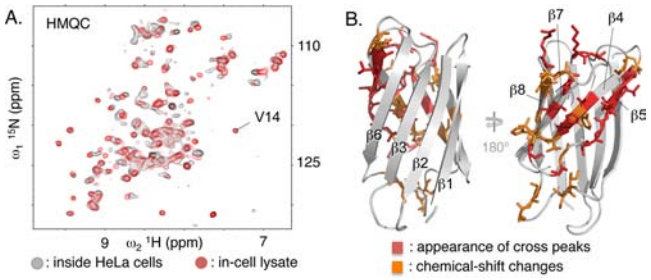

Figure 3. (A) Chemical shift differences between in-cell and lysate NMR spectra of SOD1$^{\Delta IV\ \Delta VII}$. (B) Structural location of the chemical shift differences: the effect is contained to the dynamic-sheet supporting the active site.

internalization was done in the absence of pyrenebuturate, favoring endocytosis. The procedure results in granular protein localization and fails to produce in-cell NMR spectra (S5).

A notable feature of the in-cell NMR spectrum of SOD1$^{\Delta IV\Delta VII}$ is a general broadening of the HMQC cross-peaks (Figure 3): the line width changes from 34 Hz in aqueous buffer to 51 Hz inside HeLa cells. The most apparent explanation for this broadening is decreased rotation-correlation time of the SOD1$^{\Delta IV\Delta VII}$ molecule due to diffuse interactions with other cellular components, e.g., as a result of crowding, compartmentalization, or 'electrostatic friction'. Concomitant with this general line broadening, we also observe induced chemical shifts coupled with line sharpening in specific regions of the HMQC spectrum. These shifts originate from resonances in the dynamic sheet region forming the base for the Cu-binding site (Figure 3). The induced shifts are stable over 3 h acquisition time and show no signs of heterogeneity, i.e., all of the internalized SOD1$^{\Delta IV\Delta VII}$ molecules seem to experience the same intracellular environment (S8). A straightforward explanation for the induced chemical shifts in Figure 3 would be protonation of the Cu binding His moieties in β-strands 4 and 7, i.e., the pH inside the HeLa cells is lower than that of the extracellular control. To test this idea, we acquired extracellular NMR data for SOD1$^{\Delta IV\Delta VII}$ at a series of pH values between 6.2 and 8.4 (Figure 4). The results show that acidification promotes chemical-shift changes indistinguishable from those in HeLa cells (S9). Moreover, the pH titration plots of individual resonances yield a perfect match with in-cell data at pH = 6.2 ± 0.2 (Figure 4). This consistency between titration and in-cell data shows that the spectral changes induced by cell internalization can be described by His protonation alone. The resulting intracellular pH of 6.2 ± 0.2 suggests that the cytosol of the HeLa cells acidify upon close packing in the NMR tube, most conceivably from oxygen starvation. The alternative possibility of local acidification, by endosomal or lysosomal encapsulation, is disfavored by the seemingly homogeneous NMR spectra: the span of pH values expected in the compartmentalized endosome-to-lysosome pathway would rather be seen as distorted cross-peaks. Accordingly, SOD1$^{\Delta IV\Delta VII}$ serves here as a sensitive in-cell

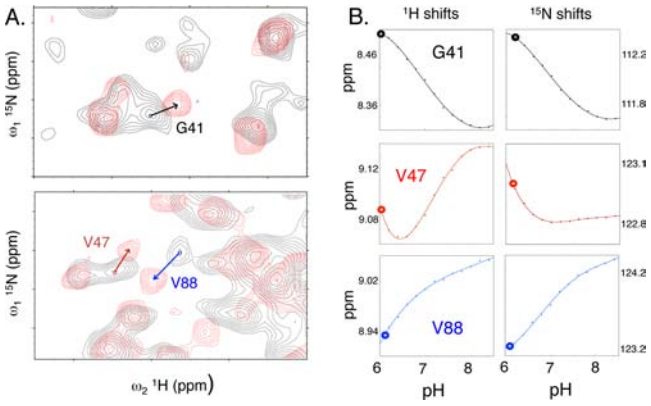

Figure 4. (A) In-cell chemical-shift changes of SOD1$^{\Delta IV\Delta VII}$ can be assigned to changes in intracellular pH. (B) Spectral differences between in-cell (gray) and lysate samples (red). *In vitro* titration of representative cross-peaks interpolated with the in-cell dittos: the uniformly aligned intersects yield an intracellular pH of 6.2 ± 0.2.

probe that lends further evidence for diffuse cytosolic localization, consistent with the fluorescence labeling in Figure 2. This straightforward strategy for pH determination is also expected to be easily applicable to other proteins as a mean to benchmark and to continuously monitor the in-cell conditions (Figure 4).

In summary, our findings show that, by rational alteration of net charge, folded SOD1 can be efficiently delivered by CPPs into mammalian cells for high-resolution in-cell NMR analysis. An advantage of this method is that it comes free of competing background of nonspecifically labeled material, which often compromises spectral resolution in approaches based on *in situ* expression. Hence, we are able to resolve the complete set of cross-peaks for the partly dynamic apoSOD1 barrel at near-physiological in-cell concentrations (Figure 2). This apo species, devoid of any stabilizing post-translational modifications, is in direct equilibrium with more unfolded and aggregation prone species[22] and is also implicated as the precursor for aggregation in ALS.[19] In the recent achievement by Banci et al. of monitoring the post-translational maturation of overexpressed SOD1 in kidney cells, the majority of NMR cross-peaks for the apo protein was found to broaden out beyond detection. As such, CPP-driven delivery of externally labeled protein, which can further be engineered to test with high spectral resolution-specific aspects of the disease mechanism, can become an important complement to *in situ* expression studies. To this end, our data show that the structure of apoSOD1$^{\Delta IV\Delta VII}$ is on the whole unaffected by the HeLa-cell interior (Figure 3); the observed spectral changes can be accounted for by His protonation alone (Figure 4). This does not exclude, however, that the protein's thermodynamic properties and conformational sampling change significantly upon subjection to the cellular interior.[23] For instance, as a result of solvent crowding,[24,25] transient encounters with other biomolecules[5,10] or active interference from the housekeeping systems maintaining function[11] and proteostasis.[26] The strategy for specific delivery of the aggregation precursor of SOD1[22] presented here could be a first step toward elucidating at structural level the role of these ubiquitous cellular factors in protein-misfolding disease.

dx.doi.org/10.1021/ja404425r | J. Am. Chem. Soc. 2013, 135, 10266−10269

■ ASSOCIATED CONTENT

Supporting Information

Figures and experimental methods. This material is available free of charge via the Internet at http://pubs.acs.org.

■ AUTHOR INFORMATION

Corresponding Author

jensd@dbb.su.se; shirakawa@moleng.kyoto-u.ac.jp; mikael@dbb.su.se

Notes

The authors declare no competing financial interest.

■ ACKNOWLEDGMENTS

Funding was from SSF (MDB10-0030), Swedish Research Council (VR 2009−5580), the Knut and Alice Wallenberg Foundation, the Bertil Hållsten Foundation and Hjärnfonden.

■ REFERENCES

(1) Zhou, H. X.; Rivas, G.; Minton, A. P. *Annu. Rev. Biophys.* **2008**, *37*, 375.
(2) Tyedmers, J.; Mogk, A.; Bukau, B. *Nat. Rev. Mol. Cell Biol.* **2010**, *11*, 777.
(3) Ebbinghaus, S.; Gruebele, M. *J. Phys. Chem. Lett.* **2011**, *2*, 314.
(4) Tochio, H. *Curr. Opin. Chem. Biol.* **2012**, *16*, 609.
(5) Binolfi, A.; Theillet, F. X.; Selenko, P. *Biochem. Soc. Trans.* **2012**, *40*, 950.
(6) Sakakibara, D.; Sasaki, A.; Ikeya, T.; Hamatsu, J.; Hanashima, T.; Mishima, M.; Yoshimasu, M.; Hayashi, N.; Mikawa, T.; Walchli, M.; Smith, B. O.; Shirakawa, M.; Guntert, P.; Ito, Y. *Nature* **2009**, *458*, 102.
(7) Banci, L.; Barbieri, L.; Bertini, I.; Luchinat, E.; Secci, E.; Zhao, Y.; Aricescu, A. R. *Nat. Chem. Biol.* **2013**, *9*, 297.
(8) Bekei, B.; Rose, H. M.; Herzig, M.; Dose, A.; Schwarzer, D.; Selenko, P. *Methods Mol. Biol.* **2012**, *895*, 43.
(9) Ogino, S.; Kubo, S.; Umemoto, R.; Huang, S.; Nishida, N.; Shimada, I. *J. Am. Chem. Soc.* **2009**, *131*, 10834.
(10) Inomata, K.; Ohno, A.; Tochio, H.; Isogai, S.; Tenno, T.; Nakase, I.; Takeuchi, T.; Futaki, S.; Ito, Y.; Hiroaki, H.; Shirakawa, M. *Nature* **2009**, *458*, 106.
(11) Banci, L.; Barbieri, L.; Bertini, I.; Cantini, F.; Luchinat, E. *PloS One* **2011**, *6*, e23561.
(12) Banci, L.; Bertini, I.; Cramaro, F.; Del Conte, R.; Viezzoli, M. S. *Biochemistry* **2003**, *42*, 9543.
(13) Leinartaite, L.; Saraboji, K.; Nordlund, A.; Logan, D. T.; Oliveberg, M. *J. Am. Chem. Soc.* **2010**, *132*, 13495.
(14) Danielsson, J.; Awad, W.; Saraboji, K.; Kurnik, M.; Lang, L.; Leinartaite, L.; Marklund, S. L.; Logan, D. T.; Oliveberg, M. *Proc. Natl. Acad. Sci. U.S.A.* **2013**, *110*, 3829.
(15) Lindberg, M. J.; Normark, J.; Holmgren, A.; Oliveberg, M. *Proc. Natl. Acad. Sci. U.S.A.* **2004**, *101*, 15893.
(16) Deshayes, S.; Morris, M.; Heitz, F.; Divita, G. *Adv. Drug Delivery Rev.* **2008**, *60*, 537.
(17) Vergunst, A. C.; van Lier, M. C.; den Dulk-Ras, A.; Stuve, T. A.; Ouwehand, A.; Hooykaas, P. J. *Proc. Natl. Acad. Sci. U.S.A.* **2005**, *102*, 832.
(18) McNaughton, B. R.; Cronican, J. J.; Thompson, D. B.; Liu, D. R. *Proc. Natl. Acad. Sci. U.S.A.* **2009**, *106*, 6111.
(19) Lang, L.; Kurnik, M.; Danielsson, J.; Oliveberg, M. *Proc. Natl. Acad. Sci. U.S.A.* **2012**, *109*, 17868.
(20) Danielsson, J.; Kurnik, M.; Lang, L.; Oliveberg, M. *J. Biol. Chem.* **2011**, *286*, 33070.
(21) Austin, C. D.; Wen, X.; Gazzard, L.; Nelson, C.; Scheller, R. H.; Scales, S. J. *Proc. Natl. Acad. Sci. U.S.A.* **2005**, *102*, 17987.
(22) Nordlund, A.; Oliveberg, M. *Proc. Natl. Acad. Sci. U.S.A.* **2006**, *103*, 10218.
(23) Guo, M.; Xu, Y.; Gruebele, M. *Proc. Natl. Acad. Sci. U.S.A.* **2012**, *109*, 17863.
(24) Waudby, C. A.; Mantle, M. D.; Cabrita, L. D.; Gladden, L. F.; Dobson, C. M.; Christodoulou, J. *J. Am. Chem. Soc.* **2012**, *134*, 11312.
(25) Gershenson, A.; Gierasch, L. M. *Curr. Opin. Struct. Biol.* **2011**, *21*, 32.
(26) Ong, D. S.; Kelly, J. W. *Curr. Opin. Cell Biol.* **2011**, *23*, 231.